

Fast Solvers for Wave Propagation problems

Victorita Dolean

Contents

1	Helmholtz Equation: Modeling, Discretization, and Solvers	1
1.1	Time-Harmonic Reduction and Wave Number	2
1.2	Discretization Methods: FD vs FE	3
1.3	Solving the Discrete System	4
2	Domain Decomposition and Coarse Spaces	4
2.1	One- and Two-Level Preconditioners	4
2.2	Grid-Based Coarse Space (Grid CS)	5
2.3	Summary of Two-Level Preconditioners	6
3	Numerical Experiments and Benchmarks	7
3.1	Benchmark Configurations and Solver Comparisons	7
3.2	Geophysical Benchmarks and Scalability	8
3.3	Time vs Frequency Domain	10
4	What about Maxwell?	11
4.1	Low-Frequency problems: formulation, discretisation and block preconditioner	11
4.2	Fictitious Space Lemma and Applications to Coarse Space Construction	12
4.3	Numerical Results: Geometry and Heterogeneity	14

1 Helmholtz Equation: Modeling, Discretization, and Solvers

Two examples of applications where frequency-domain equations are encountered are electromagnetic and acoustic wave modeling:

In medical imaging, one seeks to reconstruct the electrical permittivity ε by measuring the response to an incident electromagnetic field. This leads to a time-harmonic Maxwell system:

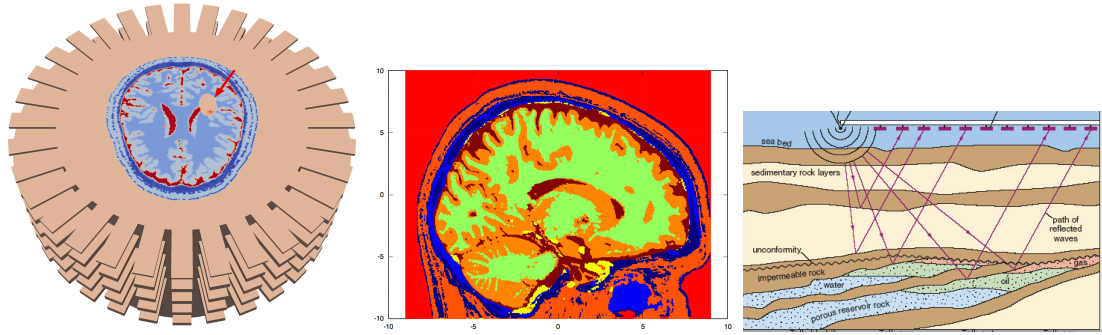
$$\nabla \times (\mu^{-1} \nabla \times \mathbf{E}) - \omega^2 \varepsilon \mathbf{E} = \mathbf{J},$$

where μ is the magnetic permeability and \mathbf{E} the electric field.

In seismic imaging, the objective is to recover subsurface parameters from scattered acoustic waves. Under a time-harmonic ansatz, the scalar wave equation reduces to the Helmholtz equation:

$$-\Delta u - \left(\frac{\omega^2}{c^2} \right) u = f,$$

where c is the local wave speed.



These applications motivate the development of accurate and scalable solvers for frequency-domain wave problems.

1.1 Time-Harmonic Reduction and Wave Number

Assuming a monochromatic source $f(x, t) = f(x)e^{-i\omega t}$, the wave solution can be written as $v(x, t) = u(x)e^{-i\omega t}$. This leads to a stationary PDE for u :

$$-\Delta u - n(x)^2 \omega^2 u = f, \quad \text{where } n(x) = \frac{1}{c(x)} \quad \Rightarrow \quad k^2(x) = n^2(x) \omega^2.$$

Oscillatory Nature of the Solution

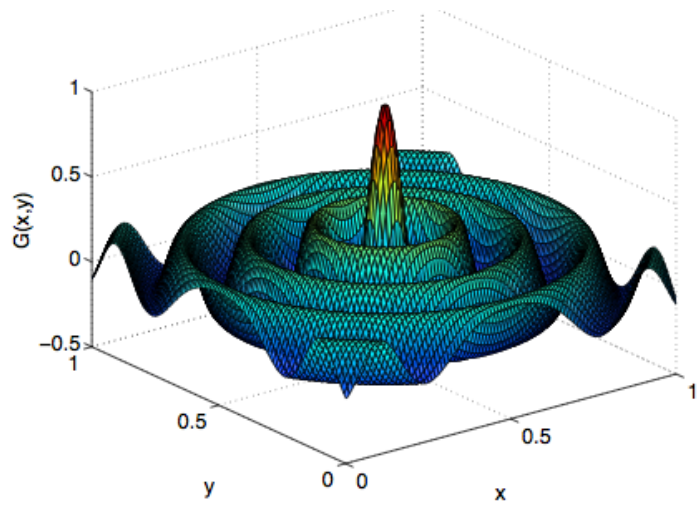
If k is small, the problem resembles a Poisson equation. For large k , the solution becomes highly oscillatory, which introduces both analytical and numerical difficulties.

Helmholtz solutions have wavelength $\lambda \sim 1/k$. To resolve such oscillations, the mesh size h must be sufficiently small and decrease at least linearly with the wavenumber. However, the required condition is more stringent:

Pollution Effect and Resolution Condition

Keeping the quantity $h\omega$ constant is insufficient to control the error. The so-called pollution effect leads to error growth with ω . For quasi-optimal accuracy with p -th order FEM, one needs:

$$h^p \omega^{p+1} \lesssim 1.$$



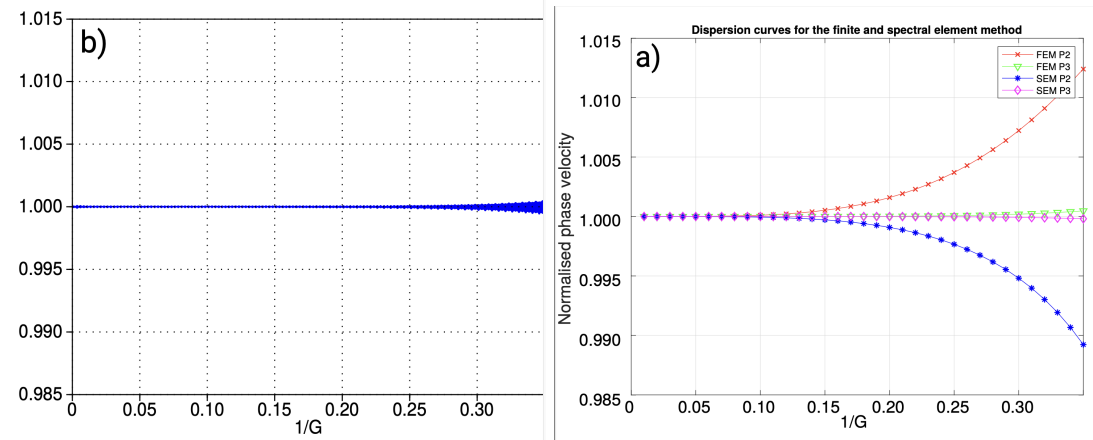
Consequences for Meshing and Approximation

- To resolve the oscillations: $h \sim 1/\omega$
- To mitigate pollution: $h \ll 1/\omega \Rightarrow h \sim \omega^{-1-1/p}$
- Trade-off: number of points per wavelength (ppwl) vs. approximation order p

1.2 Discretization Methods: FD vs FE

Two major numerical strategies are employed for solving the Helmholtz equation: finite differences and finite elements.

Finite difference (FD) methods are based on structured grids and replace differential operators with local difference operators. They offer high-order accuracy with a minimal stencil and excellent sparsity of the resulting matrix. Moreover, FD schemes can be tuned to minimize dispersion errors through coefficient optimization. This makes them especially attractive in homogeneous or smoothly varying media.



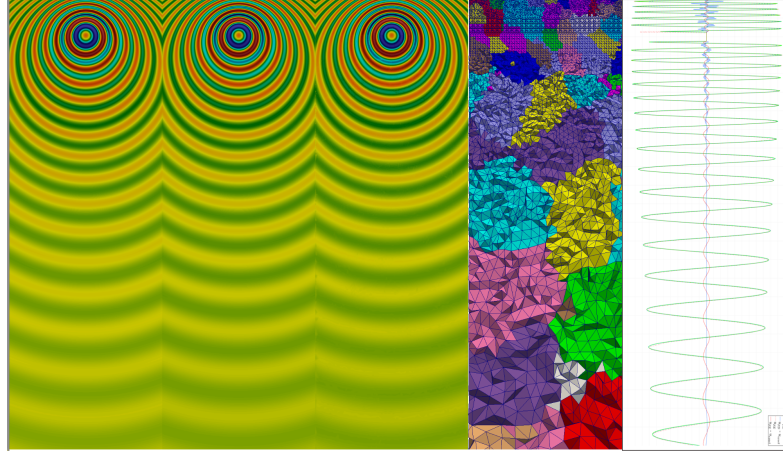
By contrast, finite element (FE) methods are built on variational formulations and are well-suited to complex geometries and heterogeneous coefficients. The ability to locally refine the mesh (*h*-adaptivity) allows FE schemes to capture fine-scale features, such as geological layers or abrupt material interfaces, while maintaining global sparsity.

While FD excels in structured, regular domains with smooth solutions, FE provides geometric flexibility and adaptivity. Both approaches have trade-offs in terms of accuracy, complexity, and implementation, however optimised finite difference schemes have better dispersion properties.

To compare the practical performance of both methods, consider a test problem with a velocity gradient in depth, using the same number of points per wavelength (4 ppwl):

Table 1: Comparison of FD and FE for increasing heterogeneity

α	λ_{\min}	λ_{\max}	#DoF FD	#DoF FE	Error FD	Error FE
0.8	125	1200	13M	28M	0.0079	0.034
2.0	125	3125	13M	16M	0.044	0.034



Left: FD and FE solutions. Right: FE mesh and vertical profile comparison.

Interpretation

Although both methods can achieve comparable error levels, finite difference (FD) methods do so with significantly fewer degrees of freedom in certain regimes. This results in lower memory usage and computational cost.

1.3 Solving the Discrete System

The discrete Helmholtz problem leads to a large, sparse, and indefinite linear system $A\mathbf{u} = \mathbf{b}$. As frequency increases, the number of degrees of freedom grows rapidly.

Solver Considerations

- A is indefinite and poorly conditioned
- $n = \#\text{DoF} \sim \omega^{(1+1/p)d}$
- Krylov solvers (GMRES, BiCGStab) struggle without preconditioning
- Direct solvers are costly in 3D

Direct Solver Complexity in 3D

	$d = 1$	$d = 2$	$d = 3$
Dense	$\mathcal{O}(n^3)$	$\mathcal{O}(n^3)$	$\mathcal{O}(n^3)$
Band	$\mathcal{O}(n)$	$\mathcal{O}(n^2)$	$\mathcal{O}(n^{7/3})$
Sparse	$\mathcal{O}(n)$	$\mathcal{O}(n^{3/2})$	$\mathcal{O}(n^2)$

2 Domain Decomposition and Coarse Spaces

2.1 One- and Two-Level Preconditioners

To solve the Helmholtz problem at high frequencies, direct solution of the large indefinite linear system is computationally challenging. Preconditioned Krylov subspace methods, particularly GMRES, are typically used to improve convergence. Domain decomposition preconditioners provide a scalable way to precondition such problems.

The classical one-level domain decomposition preconditioner takes the form:

$$M^{-1} = \sum_{j=1}^N R_j^T D_j A_j^{-1} R_j,$$

where:

- R_j : restriction operator to the subdomain Ω_j
- R_j^T : prolongation (transpose of restriction)
- D_j : diagonal matrix ensuring partition of unity
- A_j : local stiffness matrix for a subdomain Helmholtz problem with Robin boundary conditions

This approach, known as a one-level method, allows for independent solves on each subdomain. However, it suffers from poor scalability: only neighboring subdomains communicate, and information does not propagate globally.

Why One-Level is Insufficient

Due to the localized nature of subdomain solves, the iteration count increases with the number of subdomains. This is a bottleneck for large-scale problems.

Two-Level Method with Coarse Correction

To overcome this limitation, a second-level correction is introduced via a coarse space:

$$M_2^{-1} = \sum_{j=1}^N R_j^T D_j A_j^{-1} R_j + Z E^{-1} Z^*,$$

where Z spans the coarse space and $E = Z^* A Z$ is the coarse matrix. The added term ensures global information exchange, improving convergence.

Coarse Space Correction

$$M_0^{-1} = Z E^{-1} Z^*$$

This additive correction is essential for scalability.

2.2 Grid-Based Coarse Space (Grid CS)

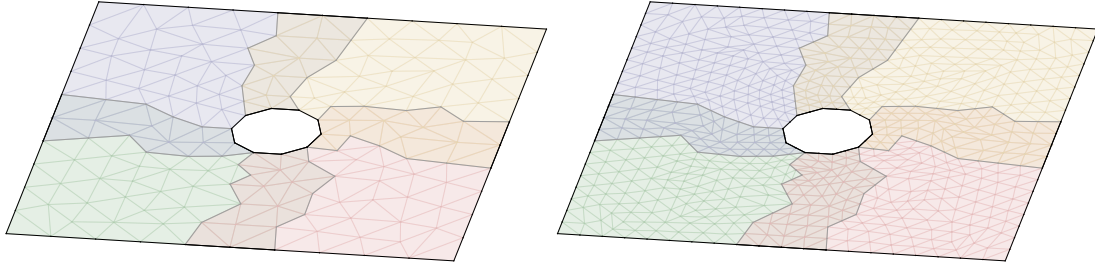
One approach to construct the coarse space is to use a geometrical coarse mesh with diameter H_{coarse} . The matrix R_0^T interpolates from fine to coarse mesh, and the coarse matrix is $E = Z^T A Z$ with $Z = R_0^T$.

The Grid Coarse Space

- Based on a coarse geometrical mesh
- $Z = R_0^T$ spans the coarse space
- $E = Z^T A Z$ is the Galerkin projection

Absorptive Problem Theory

For an absorptive Helmholtz problem (e.g., $-\Delta - (k^2 + i\xi)$), theory shows that Grid CS is effective if $H_{\text{coarse}} \sim k^{-\alpha}$ with $0 < \alpha \leq 1$ and $|\xi| \sim k^2$. In this regime, GMRES convergence becomes independent of k .



This result is due to Graham, Spence, and Vainikko and guarantees robustness in the frequency regime for the absorptive (shifted Laplacian) version of the Helmholtz equation. It has been extended to Maxwell's equations in [Dolean et al.(2019)].

Why This Theory May Be Too Pessimistic

Although the convergence theory is rigorous, it is widely considered pessimistic in practice:

- It assumes generous overlap between subdomains.
- Empirical studies show that coarser grids (i.e., larger H_{coarse}) and milder absorption $|\xi| \ll k^2$ often suffice.
- These theoretical conditions may overestimate the required coarse space size to achieve robustness.

This mismatch has motivated the development of alternative coarse spaces such as DtN and GenEO, which offer improved efficiency and adaptivity.

2.3 Summary of Two-Level Preconditioners

In general, a two-level domain decomposition preconditioner for the Helmholtz equation takes the form:

$$M_2^{-1} = \sum_{j=1}^N R_j^T D_j A_j^{-1} R_j + Z(Z^* A Z)^{-1} Z^*.$$

The choice of the coarse space Z is crucial and defines the performance and robustness of the method. We summarize three common constructions:

(1) Grid Coarse Space (Grid CS) A classical choice where Z is constructed from a coarse finite element mesh with diameter H_{coarse} . Let R_0^T denote the interpolation matrix from the coarse grid to the fine grid, then:

$$Z = R_0^T, \quad E = Z^T A Z.$$

This approach is simple to implement and supported by theory in absorptive settings.

(2) Dirichlet-to-Neumann Coarse Space (DtN CS) Based on local spectral decompositions of the Dirichlet-to-Neumann map. For each subdomain Ω_j , solve:

$$\text{DtN}_{\Omega_j}(u_{\Gamma_j}^l) = \lambda^l u_{\Gamma_j}^l,$$

where $u_{\Gamma_j}^l$ are interface modes. Each coarse basis function is then extended harmonically in the subdomain and globally assembled as:

$$Z = R_j^T D_j \mathcal{H}(u_{\Gamma_j}^l).$$

(3) Generalized Eigenproblems in the Overlap (GenEO) A robust and theoretically grounded approach that solves local generalized eigenvalue problems. For example, we can use the modes generated via the Laplace operator:

$$L_j \mathbf{u}_j^l = \lambda^l D_j L_j D_j \mathbf{u}_j^l,$$

or those for the Helmholtz operator (\mathcal{H}_k -GenEO):

$$\tilde{B}_j \mathbf{u}_j^l = \lambda^l D_j B_{j,k} D_j \mathbf{u}_j^l.$$

The resulting coarse basis vectors are extended globally as:

$$Z = R_j^T D_j \mathbf{u}_j^l.$$

These constructions are adaptive to heterogeneity and lead to a frequency robust performance. While the use of Laplace

Summary of Available Results

- **Grid CS:** Well-established theory for absorptive Helmholtz ($k^2 + i\xi$), robust if $H \sim k^{-\alpha}$ for $0 < \alpha \leq 1$.
- **Δ -GenEO:** Robust for mild heterogeneities and low frequencies; good theoretical support.
- **\mathcal{H}_k -GenEO:** Effective in high-frequency and indefinite cases; strong numerical evidence, theoretical results difficult, partial results available.

3 Numerical Experiments and Benchmarks

This section presents a range of numerical experiments designed to evaluate the performance and scalability of domain decomposition preconditioners for high-frequency wave propagation problems. The simulations are performed using the open-source **FreeFem++** library with the **ffddm** plugin and the **hpddm** C++/MPI solver backend. We focus on complex benchmarks arising in electromagnetics and geophysics.

3.1 Benchmark Configurations and Solver Comparisons

We consider four representative problems:

- The 2D and 3D **COBRA** cavity test cases for electromagnetic resonance.
- The **Marmousi** model for layered acoustic wave propagation.
- The **Overthrust** model, a geophysical benchmark.

Each problem is solved using three different coarse space strategies:

1. **Grid Coarse Space (Grid CS):** Based on a structured coarse mesh.
2. **H-GenEO:** Spectral coarse space constructed from local eigenproblems.
3. **DtN:** Dirichlet-to-Neumann coarse space using local interface eigenmodes.

The table below summarizes the performance of each coarse space under increasing resolution: 5 or 10 points per wavelength (ppwl), for both low- and high-frequency regimes.

Problem	d	freq	Grid CS		H-GenEO		DtN	
			5 ppwl	10 ppwl	5 ppwl	10 ppwl	5 ppwl	10 ppwl
Marmousi	2D	low	✓	✓	✓	✓	✓✓	✓✓
		high	✓✓	✓	✗	✓✓	✓	✓
COBRA Cavity	2D	low	✓	✓	✗	✗	✓✓	✓✓
		high	✗	✓	✗	✗	✓✓	✓✓
COBRA Cavity	3D	low	✓	✓✓	✗	✗	✓✓	✓
		high	✗	✓✓	✗	✗	✓✓	✓
Overthrust	3D	low	✓	✓	✗	✓	✓	✓
		high	✓	✓	✗	✓	✓	✓

These results are based on the comparison in [?], which provides detailed evaluations of coarse spaces in the high-frequency regime. The grid coarse space was then retained for further testing in more realistic configurations.

3.2 Geophysical Benchmarks and Scalability

To assess the scalability and efficiency of frequency-domain Helmholtz solvers in realistic settings, a suite of geophysical benchmarks was designed. All tests consider isotropic acoustic wave propagation. The main models include:

- **Homogeneous:** A $10 \text{ km} \times 20 \text{ km} \times 10 \text{ km}$ cube with constant wave speed.
- **Linear:** A domain with the same dimensions as above, but with linearly increasing wave speed in the y -direction.
- **Overthrust:** The SEG/EAGE Overthrust model ($20 \times 20 \times 4.65 \text{ km}$), a classical test case with moderate heterogeneity.
- **GO_3D_OBS:** A highly heterogeneous crustal geomodel from Tournier et al. [?], covering $20 \times 102 \times 28.4 \text{ km}$, specifically crafted to challenge seismic imaging workflows.

Table 2: Summary of benchmark properties

Model	c_m (m/s)	c_M (m/s)	f (Hz)	λ_{min}	λ_{max}	G_m	G_M	N_λ
Homogeneous	1500	1500	7.5	200	200	4	4	100
Linear	1500	8500	7.5	200	1133	4	22.7	50
Overthrust	2179	6000	10	218	600	4.4	12	50
GO_3D_OBS	1500	8639	3.75	400	2303	4	23	255

Mesh and Velocity Field: GO_3D_OBS The crustal model GO_3D_OBS includes realistic geological interfaces such as bathymetry and sediment layering. An adapted mesh is used to match the wavelength distribution. At 3.75 Hz, the adapted tetrahedral mesh consists of approximately 132 million elements, while a uniform grid would require 402.4 million cells — yielding a coarsening factor of about 3.

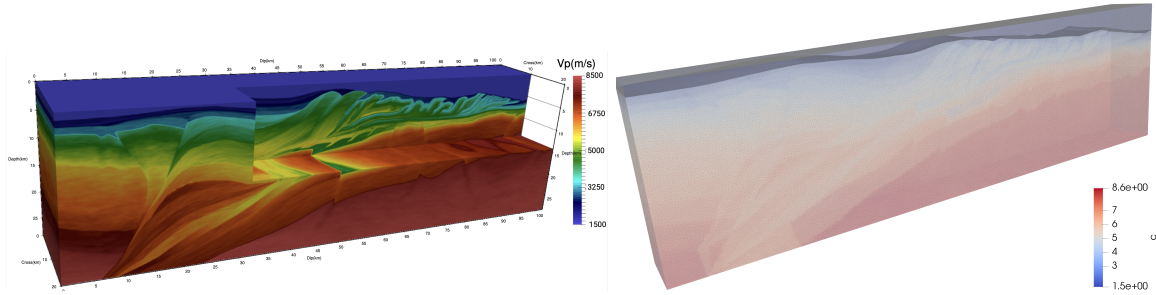


Figure 1: Velocity field of the GO_3D_OBS crustal model (left), Adapted mesh conforming to bathymetry (right)

Scalability Results: Frequency Sweep A weak scaling experiment on the GO_3D_OBS model using a finite difference discretization demonstrates the effect of frequency on both solver iteration counts and total run times. To be mentioned that due to the frequency and large number of degrees of freedom, finite difference methods are preferred to finite elements.

Table 3: Weak scalability: iteration count and timings with increasing frequency

f (Hz)	#dof (10 ⁶)	#cores	#it	ovl	T_f (s)	T_s (s)	T_{tot} (s)	E_w
2.5	21.4	60	26	3	52.5	24.8	77.3	1
3.75	67.5	360	40	3	21.9	18.6	40.5	1.003
5.0	153.5	875	61	3	20.9	26.0	46.9	0.811
7.5	500.1	2450	98	4	26.7	60.8	87.5	0.506
10.0	1160.6	9856	142	5	15.1	70.8	85.9	0.297

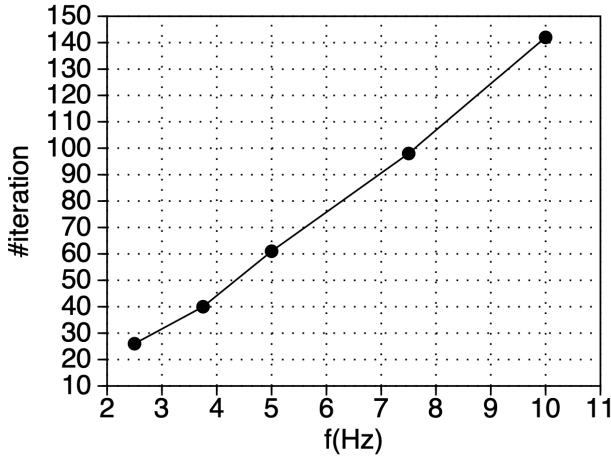


Figure 2: Iteration count vs. frequency in weak scaling

Strong Scalability: FD vs FE at 3.75 Hz At 3.75 Hz, we compare strong scalability for both finite difference (FD) and finite element (FE) discretizations:

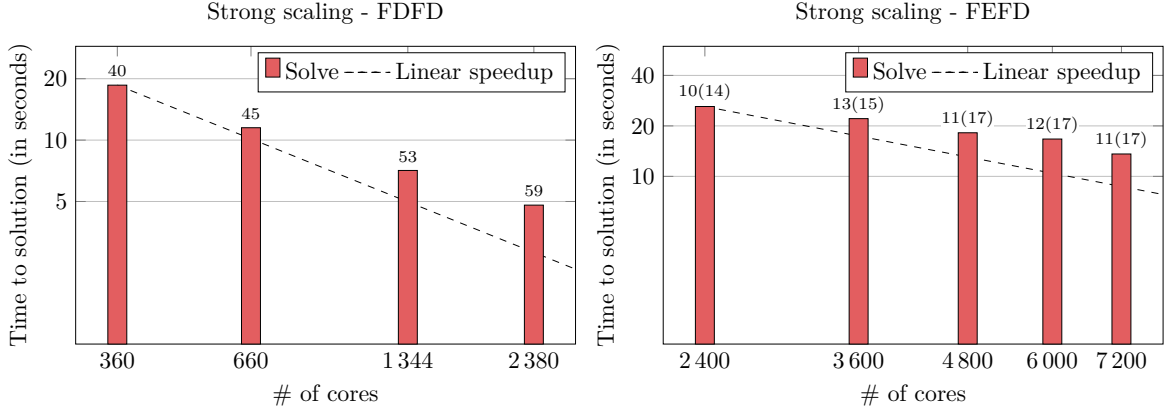


Figure 3: FD case (67.5M dofs) (left) and FE case (597.7M dofs) (right)

In both settings, the solver scales well, with almost linear speedup.

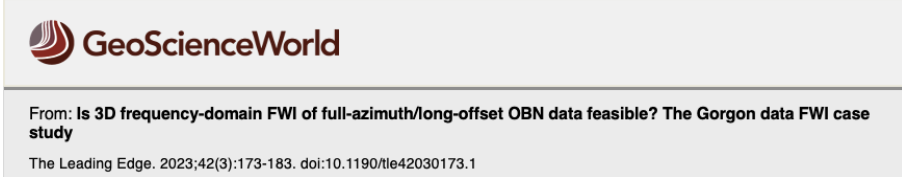
3.3 Time vs Frequency Domain

Finally, a direct comparison is made between a classical FDTD solver and frequency-domain solvers (MUMPS, ORAS) for 130 RHS:

Table 4: Wall-clock hours for solving 130 RHSs at 3.75 Hz

FDTD			MUMPS					ORAS		
#cores	$T_s^{(130)}$ (s)	T_{hc} (hr)	#c	T_f	T_s^1	T_s^{130}	T_{hc}	#c	T_s^{130}	T_{hc}
12480	264	915	1920	1000	3.9	28.3	548	1344	256.8	96

Despite the high memory footprint, the frequency-domain solver outperforms the time-domain one in total hours-to-solution. These results confirm that such solvers can serve as efficient forward engines for full-waveform inversion (FWI).



The numerical solution of the Helmholtz equation at high frequencies remains one of the most challenging tasks in scientific computing due to the rapid growth in complexity with frequency. However, recent developments have enabled the design of efficient, accurate, and scalable forward solvers, particularly in the context of 3D frequency-domain full waveform inversion (FWI). Among these, finite-difference methods (FDFD) have demonstrated superior computational efficiency compared to finite elements (FEFD), provided the mesh structure and geometry allow it. The current framework supports real-world applications such as crustal-scale seismic imaging, where large-scale heterogeneous models must be handled. Two major research directions emerge: (i) further deployment of these solvers as engines for visco-acoustic FWI in 3D, and (ii) extensions to more complex visco-elastic formulations. From a theoretical standpoint, the behavior of some methods remains insufficiently understood, highlighting the need for deeper mathematical insight, possibly through microlocal analysis or operator theory. On the computational side, strategies to reduce the number of forward solves—such as surrogate modeling or learning-based approaches—could significantly improve the viability of inversion workflows.

4 What about Maxwell?

James Clerk Maxwell (1831–1879), a Scottish mathematician and physicist, laid the foundation for classical electromagnetism through his unifying equations, which remain fundamental to modern physics and engineering. His legacy is celebrated in his hometown of Edinburgh, where the Royal Society of Edinburgh has dedicated a room to his memory, displaying his manuscripts, a hologram, and a portrait. Additionally, a public statue on George Street commemorates Maxwell alongside his dog, with an engraved plaque highlighting his famous equations. These memorials reflect not only historical reverence but also the lasting impact of Maxwell's work on contemporary fields such as scientific computing, wave propagation, and electromagnetic simulation.



4.1 Low-Frequency problems: formulation, discretisation and block preconditioner

Maxwell's equations in the time-harmonic regime describe the behavior of electromagnetic fields and are central to numerous applications such as waveguides, geophysical imaging, and microwave cavities. In the low-frequency regime (i.e., $\omega \ll 1$), these equations become nearly singular and require special formulation and numerical treatment.

To maintain stability and satisfy the divergence constraint, a mixed formulation is employed. Following [Li et al. (2012)], the problem is written as:

$$\begin{aligned} \nabla \times (\mu^{-1} \nabla \times \mathbf{E}) - \omega^2 \epsilon \mathbf{E} + \epsilon \nabla p &= \mathbf{f} \quad \text{in } \Omega, \\ \nabla \cdot (\epsilon \mathbf{E}) &= 0 \quad \text{in } \Omega, \\ \mathbf{E} \times \mathbf{n} &= 0 \quad \text{on } \partial\Omega, \\ p &= 0 \quad \text{on } \partial\Omega, \end{aligned}$$

where \mathbf{E} is the electric field, p is an auxiliary scalar field, μ is the magnetic permeability, and ϵ is the electric permittivity.

Purpose of the Mixed Form

- Stabilizes the formulation in the low-frequency limit.
- Ensures compliance with the divergence-free condition.
- Enables use of robust finite element discretization.

Discretizing the problem with Nédélec edge elements for \mathbf{E} and Lagrange elements for p yields a saddle point system:

$$\begin{pmatrix} K - \omega^2 M & B^T \\ B & 0 \end{pmatrix} \begin{pmatrix} \mathbf{E} \\ \mathbf{p} \end{pmatrix} = \begin{pmatrix} \mathbf{f} \\ 0 \end{pmatrix},$$

where:

- K is the discretized curl-curl operator $\nabla \times (\mu^{-1} \nabla \times \cdot)$, possibly with a large kernel.
- M is the mass matrix weighted by ε .
- B enforces the divergence constraint.

Due to the indefiniteness of the system, a block-diagonal preconditioner is used:

$$\mathcal{P}_{M,L} = \begin{pmatrix} \mathcal{P}_M & 0 \\ 0 & L \end{pmatrix}, \quad \mathcal{P}_M = K + \gamma M, \quad \gamma = 1 - \omega^2 > 0,$$

where L is an ε -weighted Laplacian. The operator \mathcal{P}_M regularizes the curl-curl operator and is critical in ensuring efficient convergence.

Preconditioning Challenge

Key issue: Efficient solution of the positive-definite Maxwell problem:

$$\nabla \times (\mu^{-1} \nabla \times \mathbf{E}) + \gamma \varepsilon \mathbf{E} = \mathbf{f},$$

with boundary condition $\mathbf{E} \times \mathbf{n} = 0$ on $\partial\Omega$.

AMS Preconditioner

The auxiliary space Maxwell solver (AMS) [Hiptmair and Xu(2007)], available via PETSc, is a robust preconditioner that leverages nodal auxiliary spaces to handle the large kernel of K . It is especially effective in low-frequency regimes and has been recognized as a major computational breakthrough [DOE report (2008)].

4.2 Fictitious Space Lemma and Applications to Coarse Space Construction

The Fictitious Space Lemma (FSL), introduced by Nepomnyaschikh [Nepomnyaschikh(1991)], provides a powerful theoretical tool for the analysis and design of preconditioners based on auxiliary or enriched function spaces.

Let \mathcal{H}_O and \mathcal{H}_P be Hilbert spaces endowed with symmetric positive definite bilinear forms $a(\cdot, \cdot)$ and $b(\cdot, \cdot)$, respectively. Let $A : \mathcal{H}_O \rightarrow \mathcal{H}_O$ and $B : \mathcal{H}_P \rightarrow \mathcal{H}_P$ denote the Riesz maps induced by these bilinear forms:

$$\begin{aligned} a(u, v) &= (Au, v), \quad \forall u, v \in \mathcal{H}_O, \\ b(u_D, v_D) &= (Bu_D, v_D), \quad \forall u_D, v_D \in \mathcal{H}_P. \end{aligned}$$

Assume there exists a linear and surjective mapping $\mathcal{R} : \mathcal{H}_P \rightarrow \mathcal{H}_O$. The lemma assumes:

- **Continuity:** There exists $c_R > 0$ such that

$$a(\mathcal{R}u_D, \mathcal{R}u_D) \leq c_R b(u_D, u_D), \quad \forall u_D \in \mathcal{H}_P.$$

- **Stable Decomposition:** There exists $c_T > 0$ such that for every $u \in \mathcal{H}_O$, there exists $u_D \in \mathcal{H}_P$ with $\mathcal{R}u_D = u$ and

$$b(u_D, u_D) \leq \frac{1}{c_T} a(u, u).$$

Define the adjoint $\mathcal{R}^* : \mathcal{H}_O \rightarrow \mathcal{H}_P$ by:

$$(\mathcal{R}u_D, u) = (u_D, \mathcal{R}^*u)_D, \quad \forall u_D \in \mathcal{H}_P, u \in \mathcal{H}_O.$$

Fictitious Space Lemma

The preconditioned operator $\mathcal{R}B^{-1}\mathcal{R}^*A$ satisfies:

$$c_T a(u, u) \leq a(\mathcal{R}B^{-1}\mathcal{R}^*Au, u) \leq c_R a(u, u), \quad \forall u \in \mathcal{H}_O$$

which implies a condition number estimate:

$$\kappa_2(\mathcal{R}B^{-1}\mathcal{R}^*A) \leq \frac{c_R}{c_T}$$

The Near Kernel Coarse Space A practical application of the FSL is in the construction of coarse spaces in domain decomposition. For symmetric problems (e.g., low-frequency Maxwell), robustness often depends on capturing the near-kernel of the local operators.

Let A be the global SPD operator, and $G \subset \mathbb{R}^{\#N}$ be a subspace approximating the near-kernel (e.g., gradients of H^1 functions). Define its restriction to subdomains as $G_i = R_i G$, and set

$$V_G := \text{span} \left\{ R_i^T D_i G_i \right\}_{i=1}^N.$$

Let Z be a matrix whose columns form a basis of $V_0 := V_G$. The coarse space matrix is

$$E := Z^T A Z.$$

Application of FSL to AS Preconditioner

Define $\mathcal{H}_P = \mathbb{R}^{n_0} \times \prod_{i=1}^N \mathbb{R}^{n_i}$ and

$$\mathcal{R}_{AS}(\mathcal{U}) := ZU_0 + (I - P_0) \sum_{i=1}^N R_i^T U_i,$$

where P_0 is the A -orthogonal projection onto V_0 . Then,

$$\kappa_2(\mathcal{R}_{AS}B^{-1}\mathcal{R}_{AS}^*A) \leq (1 + C\tau_0)C'$$

with constants depending on the overlap and spectral properties of the local solves.

Extension to NK-GenEO To improve robustness in highly heterogeneous media, one can enrich V_G with spectral information from a local generalised eigenproblem orthogonal to G_i . For each subdomain j :

$$(I - \xi_{0j}^T) D_j R_j A R_j^T D_j (I - \xi_{0j}) V_{jk} = \lambda_{jk} \tilde{A}_j V_{jk}.$$

Let V_{GenEO}^τ be the space generated by eigenvectors with $\lambda_{jk} > \delta$, and define $V_0 := V_G + V_{\text{GenEO}}^\tau$.

NK-GenEO Condition Number

Let Z span V_0 , then:

$$\kappa_2(\mathcal{R}_{AS,2} B^{-1} \mathcal{R}_{AS,2}^* A) \leq (1 + C\delta) C'$$

where δ is a user-defined eigenvalue threshold.

4.3 Numerical Results: Geometry and Heterogeneity

All numerical experiments were conducted using the open-source domain-specific language **FreeFEM**, as part of the study in [Bootland et al.(2024)]. The objective is to assess and compare a range of preconditioners for low-frequency Maxwell problems under varying conditions of domain geometry and physical heterogeneity.

We focus on six strategies:

- **AMS**: Auxiliary-space Maxwell solver of Hiptmair and Xu;
- **AS**: One-level additive Schwarz;
- **AS-SNK**: Two-level additive Schwarz with split near-kernel coarse space;
- **AS-SNK-GenEO**: AS-SNK enriched with local GenEO eigenmodes;
- **AS-NK**: Two-level AS with a global near-kernel space;
- **AS-NK-GenEO**: Global NK enriched with GenEO eigenmodes.

Geometry Effects

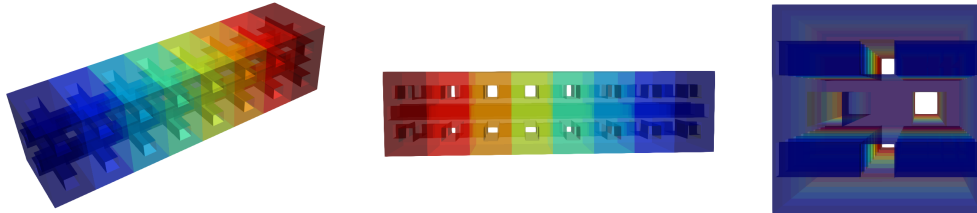


Figure 4: Non-convex beam geometry with embedded holes used for testing scalability.

Table 5 presents a weak scalability analysis with increasing number of subdomains N . We observe that:

- **AS-SNK-GenEO** consistently achieves low iteration counts (23–27), independent of N ;
- **AMS** and **AS** degrade significantly with scale;
- Both **AS-NK** and **AS-SNK** are improved substantially when enriched with GenEO modes.

Table 5: A weak scalability study for the (non-convex) homogeneous beam problem with holes

N	8	16	32	64	128	256
#dofs	113K	226K	451K	901K	1800K	3600K
NK size	18K	36K	72K	144K	288K	576K
SNK size	24K	49K	99K	198K	397K	794K
GenEO size	18	42	90	186	378	762
AMS	43	67	113	321	588	1302
AS	37	61	106	173	294	557
AS-SNK	36	62	109	202	383	554
AS-SNK-GenEO	23	24	25	26	27	27
AS-NK	36	62	111	203	386	588
AS-NK-GenEO	24	25	25	28	30	37

Robustness to Parameter γ

Table 6 investigates robustness w.r.t. the preconditioning parameter γ . The performance of GenEO-enriched methods remains remarkably stable across a wide range, while AMS and one-level AS become impractical for small γ values.

Table 6: Varying the parameter γ for the (non-convex) homogeneous beam problem with holes, $N = 256$

γ	10^{-5}	10^{-4}	10^{-3}	10^{-2}	10^{-1}	1	10	10^2
GenEO size	762	762	762	762	762	762	0	0
AMS	2057	2193	1302	303	86	33	14	6
AS	618	579	557	463	150	46	15	7
AS-SNK	772	761	554	444	144	45	17	9
AS-SNK-GenEO	28	27	27	26	23	20	17	9
AS-NK	776	765	588	444	144	45	17	10
AS-NK-GenEO	51	49	37	25	24	20	17	10

Heterogeneity in ε and μ

In Table 7, the permittivity ε varies across the geometry. GenEO enrichment is not required, as the coarse spaces based on NK or SNK alone suffice.

Table 7: Heterogeneous ε and $N = 256$ subdomains.

$\varepsilon_{\text{holes}}$	10^{-4}	10^{-3}	10^{-2}	10^{-1}	1	10	10^2	10^3	10^4
GenEO size	0	0	0	0	0	0	0	0	0
AMS	12	12	12	12	12	12	13	12	12
AS	232	232	232	232	231	231	226	180	135
AS-SNK	18	18	18	18	18	17	17	16	15
AS-SNK-GenEO	18	18	18	18	18	17	17	16	15
AS-NK	42	42	42	42	42	41	38	33	24
AS-NK-GenEO	42	42	42	42	42	41	38	33	24

In contrast, Table 8 shows the case where the permeability μ is varied. GenEO is automat-

ically activated when heterogeneity increases, and it allows **AS-SNK-GenEO** and **AS-NK-GenEO** to remain stable in iteration counts, even as **AS** and **AMS** suffer.

Table 8: Heterogeneous μ and $N = 256$ subdomains.

μ_{holes}	10^{-4}	10^{-3}	10^{-2}	10^{-1}	1	10	10^2	10^3	10^4
GenEO size	0	0	0	0	0	0	762	1016	15808
AMS	18	18	16	13	12	12	20	32	43
AS	216	216	216	219	231	241	247	299	448
AS-SNK	18	18	18	18	18	23	45	119	287
AS-SNK-GenEO	18	18	18	18	18	23	26	24	25
AS-NK	39	39	39	39	42	44	53	132	299
AS-NK-GenEO	39	39	39	39	42	44	45	45	43

The GenEO-based enrichment of coarse spaces, when combined with additive Schwarz, offers excellent robustness across challenging settings: non-convex geometries, low-frequency Maxwell equations, and high contrast media. These tests confirm the relevance of fictitious space inspired domain decomposition approaches for $H(\text{curl})$ problems.

References

- [Dolean et al.(2019)] N. Bonazzoli, V. Dolean, I.G. Graham, E.A. Spence, and A. Tournier. *Domain decomposition preconditioning for the high-frequency time-harmonic Maxwell problems*, Mathematics of Computation, 88(317):2559–2604, 2019.
- [Bootland et al.(2022)] N. Bootland, V. Dolean, I.G. Graham, J. Ma, and R. Scheichl. *Overlapping Schwarz methods with GenEO coarse spaces for indefinite and nonself-adjoint problems*, IMA Journal of Numerical Analysis, 42(3):1841–1870, 2022.
- [Bootland et al.(2021)] N. Bootland, V. Dolean, P. Jolivet, and A. Tournier. *A comparison of coarse spaces for Helmholtz problems in the high frequency regime*, Computers and Mathematics with Applications, 101:180–198, 2021.
- [Tournier et al.(2022)] A. Tournier, P. Jolivet, V. Dolean, B. Aghamiry, S. Operto, and N. Riffo. *3D finite-difference and finite-element frequency-domain wave simulation: A comparative study*, Geophysics, 87(5):T273–T291, 2022.
- [Hiptmair and Xu(2007)] R. Hiptmair and J. Xu. *Nodal auxiliary space preconditioning in $H(\text{curl})$ and $H(\text{div})$ spaces*, SIAM Journal on Numerical Analysis, 45(6):2483–2509, 2007.
- [Nepomnyaschikh(1991)] S.V. Nepomnyaschikh. *Preconditioning of iterative methods for solving boundary value problems in domains with piecewise smooth boundaries*, USSR Computational Mathematics and Mathematical Physics, 31(2):42–52, 1991.
- [Bootland et al.(2024)] N. Bootland, V. Dolean, F. Nataf, and A. Tournier. *A robust and adaptive GenEO-type domain decomposition method for $H(\text{curl})$ problems in general non-convex three-dimensional geometries*, arXiv preprint arXiv:2311.18783, 2024.
- [Li et al. (2012)] J. Li, C. Greif, and D. Schötzau. A mixed finite element method for the time-harmonic Maxwell equations. *J. Comput. Appl. Math.*, 234(6):1876–1882, 2012.
- [DOE report (2008)] U.S. Department of Energy. Breakthroughs in Simulation Science, 2008.